

sufficiently for the hydrated FH...NH<sub>3</sub> prototype H-bonded system.<sup>44</sup>

The environment was modeled by adding successive layers of unit cells to the central (000) cell. This procedure leads to crystal blocks of similar shape to that of the unit cell. In the present study for both structures, two additional layers (corresponding to a crystal block containing 125 unit cells) proved to be sufficient to simulate the potential of the infinite crystal.

$V$  of eq 2 was calculated by the bond increment method<sup>45</sup> which has already been proven to be useful in the calculation of the electrostatic potential maps of small molecules<sup>45</sup> and proteins.<sup>12a,12c,46</sup> A particular advantage of this method is that very large systems can be handled since the computational work (including the construction of the wave function) is proportional to the first power of the number of bonds in the system. For unit cells which lie far from the (0,0,0) one, the electrostatic potential was replaced by a simple monopole expression which made the calculations quite cheap even for such a large system as treated here. Atomic net charges were obtained from CNDO/2 calculations.<sup>47</sup>

According to a recent work by Voogd et al.,<sup>36</sup> the CNDO/2 charges used in our calculations generally underestimate the electrostatic lattice energies of amino acid and peptide crystals. Different systematic errors were found in predicting the energy of ion-pair (error of about 100 kJ/mol) and neutral (error of about 60 kJ/mol) structures. It means that

the  $\Delta E_s$  values obtained by our calculations with CNDO/2-based charges are underestimated by about 40 kJ/mol.

The protein potential of SGPA was calculated by using the PROTOP program<sup>46</sup> with three-dimensional coordinates from Protein Data Bank.<sup>48</sup> Surface ionizable side chains were considered as fully shielded.<sup>46</sup>

**Acknowledgment.** M. C. is indebted to Prof. A. Kálmán for his support in this work. E. W. acknowledges the financial support of the Deutsche Forschungsgemeinschaft. We thank Prof. M. N. G. James and Dr. A. Sielecki (Edmonton) for some updated coordinates of active site residues of SGPA and Prof. A. Tulinsky (East Lansing, MI) for sending a manuscript prior to publication.

**Registry No. 2**, 99827-47-1; **3**, 99827-48-2; SGPA, 55326-50-6; serine protease, 37259-58-8.

**Supplementary Material Available:** Relative atomic coordinates, anisotropic thermal parameters, selected bond lengths and angles, and structure factor tables for **2** and **3** (13 pages). Ordering information is given on any current masthead page.

(48) James, M. N. G.; Sielecki, A. R. Protein Data Bank File 1983, 85SB13, 73.

(49) The premultiplier matrix of a vector is of the form

$$\begin{array}{ccc} cB & sB \cdot sC & -sB \cdot cC \\ sA \cdot sB & cA \cdot cC - sA \cdot cB \cdot sC & sA \cdot cB \cdot cC + cA \cdot sC \\ cA \cdot sB & -cA \cdot cB \cdot sC - sA \cdot cC & cA \cdot cB \cdot cC - sA \cdot sC \end{array}$$

where "s" and "c" denote sine and cosine functions of the Euler angles A, B, and C, cf.: Schilling, J. W. Ph.D. Dissertation, University of Michigan, Ann Arbor, 1968.

(44) (a) Ángyán, J.; Náray-Szabó, G. *Theoret. Chim. Acta* **1983**, *64*, 27. (b) Ángyán, J.; Náray-Szabó, G. *Acta Chim. Acad. Sci. Hung.* **1984**, *116*, 141.

(45) (a) Náray-Szabó, G. *Int. J. Quantum Chem.* **1979**, *16*, 265. (b) Náray-Szabó, G.; Grofcsik, A.; Kósa, K.; Kubinyi, M.; Martin, A. J. *Comput. Chem.* **1981**, *2*, 58.

(46) Ángyán, J.; Náray-Szabó, G. *J. Theor. Biol.* **1983**, *103*, 349.

(47) Pople J. A., Beveridge, D. L., Eds. "Approximate Molecular Orbital Theory"; McGraw-Hill: New York, 1970.

## Ultraviolet Raman Hypochromism of the Tropomyosin Amide Modes: A New Method for Estimating $\alpha$ -Helical Content in Proteins

Robert A. Copeland and Thomas G. Spiro\*

Contribution from the Department of Chemistry, Princeton University, Princeton, New Jersey 08544. Received July 23, 1985

**Abstract:** Ultraviolet resonance Raman spectra, obtained with 200-nm excitation from a H<sub>2</sub> Raman-shifted Nd:YAG laser, are recorded for tropomyosin. The intensities of the amide II and III modes, and of the amide II' mode in D<sub>2</sub>O, increase with increasing pH, as the  $\alpha$ -helical protein unfolds. A linear relationship between intensity and  $\alpha$ -helical content has been established. This relationship has been used to estimate the helix content of myoglobin, bovine serum albumin, and cytochrome *c*, good agreement being found with previous determinations from X-ray crystallography or optical rotatory dispersion. The intensity increase associated with the loss of the helical structure is attributed to the UV absorption hypochromism of  $\alpha$ -helical peptides. The molar Raman scattering factors for the amide II, II', and III modes in helical and nonhelical structures are proportional to the squares of the molar absorptivities at 190 nm, the center of the amide absorption band, establishing local resonance for these amide modes with the  $\pi$ - $\pi^*$  transition. The amide I (C=O stretching) band intensity is nearly independent of  $\alpha$ -helical content, suggesting that it is enhanced primarily via higher lying electronic transitions.

The advent of reliable high-power pulsed lasers, whose wavelengths can readily be shifted over a wide range of the electromagnetic spectrum via nonlinear optical techniques (crystal mixers and stimulated Raman shifters) has made possible the routine acquisition of Raman spectra with ultraviolet excitation. This development has opened the way to systematic exploration of the resonance Raman characteristics of UV chromophores, including the purine and pyrimidine bases of nucleic acids<sup>1-4</sup> and the aromatic side chains of proteins,<sup>5-10</sup> as well as the amide bonds of the polypeptide backbone.<sup>8-12</sup> Resonance Raman spectroscopy is a useful structure probe due to its high sensitivity (easily ex-

tending into the micromolar range) and the chromophore specificity associated with wavelength matching of the laser to a

(1) Fodor, S. P. A.; Rava, R. P.; Hays, T. R.; Spiro, T. G. *J. Am. Chem. Soc.* **1985**, *105*, 1520-1529.

(2) Ziegler, L. D.; Hudson, B.; Strommen, D. P.; Peticolas, W. L. *Biopolymers* **1984**, *23*, 2067-2081.

(3) Kubasek, W. L.; Hudson, B.; Peticolas, W. L. *Proc. Natl. Acad. Sci. U.S.A.* **1985**, *82*, 2369-2373.

(4) Fodor, S. P. A.; Spiro, T. G. *J. Am. Chem. Soc.*, in press.

(5) Rava, R. P.; Spiro, T. G. *J. Am. Chem. Soc.* **1984**, *106*, 4062-4064.

(6) Johnson, C. R.; Ludwig, M.; O'Donnell, S.; Asher, S. A. *J. Am. Chem. Soc.* **1984**, *106*, 5008-5010.

(7) Rava, R. P.; Spiro, T. G. *J. Phys. Chem.* **1985**, *89*, 1856-1861.

(8) Rava, R. P.; Spiro, T. G. *Biochemistry* **1985**, *24*, 1861-1865.

\* Author to whom correspondence should be addressed.

particular electronic transition.<sup>13</sup> In addition, new vibrational modes can appear in the resonance Raman spectrum, whose intensity is weak or vanishing in off-resonance Raman spectra. An example is the amide II vibration, a mode of mixed C–N stretching and N–H bending characters which appears strongly in infrared spectra of peptides but very weakly in Raman spectra obtained with visible excitation.<sup>14</sup> This band is strongly enhanced, however, at wavelengths close to the first allowed amide electronic transition, near 190 nm.<sup>8–12,15–17</sup>

In a recent study of cytochrome *c*,<sup>10</sup> we noted that the amide II intensity increased at pH values where the protein is believed to undergo partial unfolding, as did the absorptivity in the far-UV, and we attributed these effects to the known hypochromism of the 190-nm amide electronic transition for  $\alpha$ -helical polypeptides.<sup>18</sup> In the present study, we extend these observations to tropomyosin, a protein whose  $\alpha$ -helical content can be varied systematically by adjusting the pH.<sup>19,20</sup> A linear response to the  $\alpha$ -helical content is found for the band intensities associated with the amide II and III modes (which are mixed vibrationally) and also for the amide II' band of protein dissolved in D<sub>2</sub>O, which is particularly strong in the 200-nm RR spectrum. The molar scattering factors for helical and nonhelical fractions are found to be roughly proportional to the squares of the absorptivities at 190 nm, as expected for a local resonance with the first allowed amide electronic transition. The intensity of the amide I mode, which is C=O stretching in character, is nearly independent of  $\alpha$ -helical content, however. The enhancement of this mode is apparently due to other electronic transitions.

The intensity of the strong and well-resolved amide II' band provides a useful probe of secondary structure, as an index of  $\alpha$ -helical content. We have used it to estimate the percent  $\alpha$ -helix for myoglobin, cytochrome *c*, and bovine serum albumin and find excellent agreement with crystallographic or optical rotatory dispersion determinations. The method has a considerable advantage over optical techniques (absorption and optical activity) which are subject to interference by other chromophores absorbing in the far-UV region, e.g., aromatic side chains and prosthetic groups.<sup>21</sup> These chromophores can also contribute to the Raman spectrum, but interference is minimal since the amide II' vibration is being monitored specifically. Also, the strong absorption from the hydroxide ion interferes with optical determination at high pH, whereas Raman scattering is not affected by the hydroxide; good quality UVRR spectra of proteins have been obtained at pH as high as 13. Nonresonance Raman spectroscopy, with visible laser excitation, has been applied to the determination of the secondary structure via the frequencies and band shapes of the amide I and amide III modes.<sup>22–24</sup> Sensitivity is low, however, and the very high protein concentration required can give misleading results due to aggregation. In addition, nonresonance

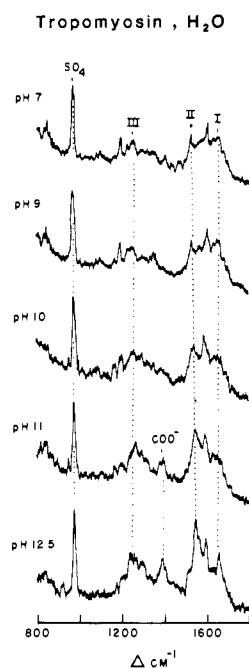


**Figure 1.** UVRR spectra of rabbit muscle tropomyosin (24  $\mu$ M in 0.05 M phosphate buffer containing 0.3 M sodium sulfate as the internal standard) excited at 200 nm at varying pH. Bands are marked for sulfate, amide modes I, II, and III, and carboxylate. See text for further details.

Raman spectra are unobtainable for proteins with prosthetic groups that absorb or fluoresce in the visible region.

#### Experimental Section

Rabbit muscle tropomyosin, sperm whale myoglobin, bovine serum albumin, and equine cytochrome *c* were purchased from Sigma and were the highest grades available. Solutions of these proteins were prepared in aqueous and D<sub>2</sub>O buffer containing 0.05 M phosphate and 0.3 M sodium sulfate. The pH/pD was monitored on a Corning Model 150 digital pH meter and was adjusted with HCl and NaOH for aqueous samples and DCl and NaOD for samples in D<sub>2</sub>O. For samples in D<sub>2</sub>O, the meter readings were corrected for the deuterium isotope effects as in ref 25. Protein samples were stored in D<sub>2</sub>O buffer for up to 1 week at 4 °C to ensure complete H/D exchange. That the amide H/D exchange was complete was evident from the lack of an amide II band (being replaced by the amide II' band) in the UVRR spectra of these samples. Tropomyosin solutions were prepared at concentrations of 24  $\mu$ M (H<sub>2</sub>O) and 18  $\mu$ M (D<sub>2</sub>O) in protein, while the other protein solutions were 200  $\mu$ M.

Ultraviolet excitation at 200 nm was provided by a frequency-doubled, mode-locked Nd:YAG (Quanta-Ray DCR-2A) pulsed laser in conjunction with a H<sub>2</sub> Raman shift cell as previously described.<sup>1</sup> The fourth harmonic output of the laser (266 nm) was directed into the H<sub>2</sub> shifter, and the third anti-Stokes shifted line was used to excite the sample. The laser light was focused onto an open stream of sample solution. The scattered light was collected by using a 135° backscattering geometry and focused onto the entrance slit (300  $\mu$ m) of a 1.26-m single monochromator (Spex 1269). The Raman scattering was detected with a solar blind photomultiplier tube (Hamamatsu UH 166) and processed with a PAR Model 162 boxcar integrator which was interfaced with a Plessey computer. This same computer was used to drive the monochromator in 0.05  $\text{\AA}/\text{s}$  steps. The reported spectra are each the sum of five to eight scans. The sample solutions were changed after every second scan to avoid any artifacts that might arise from photoinduced damage to the proteins.

The Raman intensities of the amide vibrational modes were measured as peak heights and were normalized to the intensity of the 981-cm<sup>-1</sup> band of sodium sulfate, which was added to the protein solutions as an internal standard. The intensities were converted to molar scattering ratios, *R*, by using the formula

$$R = \frac{I_N C_{\text{SO}_4}}{I_{\text{SO}_4} C_N} [A] \quad (1)$$

where *I<sub>N</sub>* is the intensity of the sample vibrational mode, *I<sub>SO<sub>4</sub></sub>* is the intensity of the sulfate Raman band, *C<sub>N</sub>* is the molar concentration of

(9) Copeland, R. A.; Dasgupta, S.; Spiro, T. G. *J. Am. Chem. Soc.* **1985**, *107*, 3370–3371.

(10) Copeland, R. A.; Spiro, T. G. *Biochemistry* **1985**, *24*, 4960–4968.

(11) Mayne, L. C.; Ziegler, L. D.; Hudson, B. J. *Phys. Chem.*, **1985**, *89*, 3395–3398.

(12) Dudik, J. M.; Johnson, C. R.; Asher, S. A. *J. Phys. Chem.*, **1985**, *89*, 3805–3814.

(13) Spiro, T. G.; Stein, P. *Ann. Rev. Phys. Chem.* **1977**, *28*, 501–521.

(14) Carey, P. R. "Biochemical Applications of Raman and Resonance Raman Spectroscopies"; Academic Press: New York, 1982, pp 71–98.

(15) Harada, I.; Sugawara, Y.; Matsuura, H.; Shimanouchi, T. *J. Raman Spectrosc.* **1975**, *4*, 91–98.

(16) Sugawara, Y.; Harada, I.; Matsuura, H.; Shimanouchi, T. *Biopolymers* **1978**, *17*, 1405–1421.

(17) Hudson, B.; Mayne, L. *Methods Enzymol.*, in press.

(18) Rosenheck, K.; Doty, P. *Proc. Natl. Acad. Sci. U.S.A.* **1961**, *47*, 1775–1785.

(19) Lowey, S. J. *Biol. Chem.* **1965**, *240*, 2421–2427.

(20) Frushour, B. G.; Koenig, J. L. *Biopolymers* **1974**, *13*, 1809–1819.

(21) Campbell, I. D.; Dwek, R. A. "Biological Spectroscopy"; Benjamin/Cummings: Menlo Park, CA, 1984; pp 255–278.

(22) Frushour, B. G.; Koenig, J. L. In "Advances in Infrared and Raman Spectroscopy"; Clark, R. J. H., Hester, R. E., Eds.; Heyden: New York, 1975; Vol. 1, pp 35–97.

(23) Williams, R. W. *J. Mol. Biol.* **1983**, *166*, 581–603.

(24) Williams, R. W. *Methods Enzymol.*, in press.

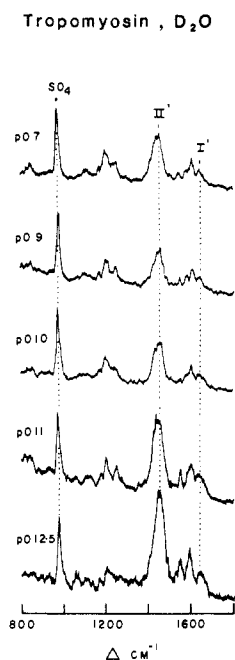


Figure 2. As Figure 1 but for D<sub>2</sub>O solutions at the indicated pD.

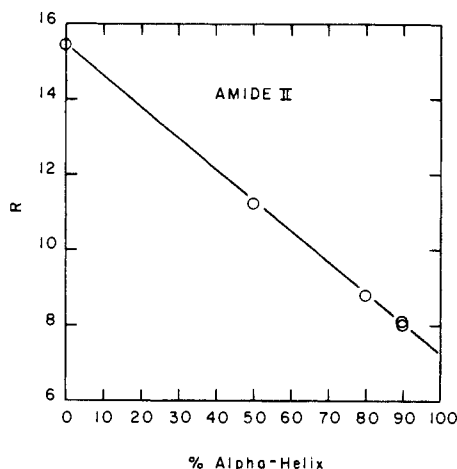


Figure 3. Plot of the molar scattering ratio for the amide II band vs.  $\alpha$ -helix content as determined by Lowey<sup>19</sup> for rabbit muscle tropomyosin in H<sub>2</sub>O.

peptide bonds in the sample,  $C_{SO_4}$  is the molar concentration of sodium sulfate, and  $A$  is a correction term for sample absorption, as described by Fodor et al.<sup>1</sup> Since the sulfate and the amide vibrational modes are close in wavelength, the correction for the absorption was small and could be neglected. The reported scattering ratios are averages over two to four determinations.

### Results

UVRR spectra are shown in Figures 1 and 2 for tropomyosin in H<sub>2</sub>O and D<sub>2</sub>O solution at pH/pD values of 7.0, 9.0, 10.0, 11.0, and 12.5. Table I lists the band frequencies and assignments. The  $\alpha$ -helix content of the protein is known<sup>19,20</sup> to decrease from 90% to 0% over this range. It is clear that the intensities of the amide II and the amide III bands in H<sub>2</sub>O and the amide II' band in D<sub>2</sub>O (labeled in the figures) increase with increasing pH. The frequencies of the amide III and amide I, or I', bands are also affected by increasing the pH (see Table I) in a direction consistent with lower  $\alpha$ -helix content for the high pH forms. The intensity of the amide I or I' bands, however, appears to be unaffected by pH. These results are more clearly illustrated in Figures 3–5 which show plots of the amide band intensities against percent  $\alpha$ -helix as determined by Lowey.<sup>19</sup> Although there is some scatter in the points, the least-squares straight lines give a satisfactory account of the relationship ( $\geq 99\%$  confidence level for all plots except amide I which showed no correlation).

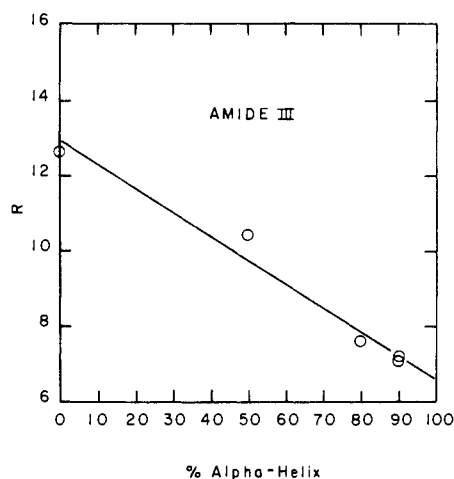


Figure 4. As Figure 3 but for the amide III band.

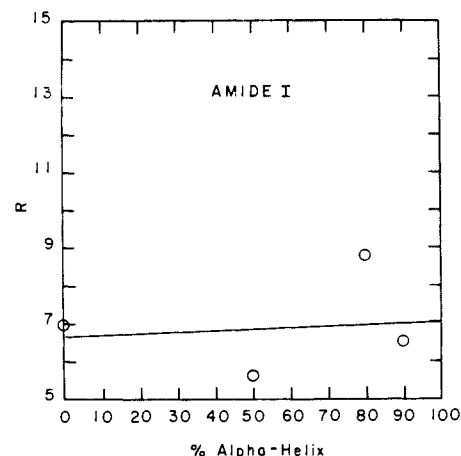


Figure 5. As Figure 3 but for the amide I band. The circle at 90%  $\alpha$ -helix represents two data points, pH 7 and pH 9, whose  $R$  values were practically identical (see Table II).

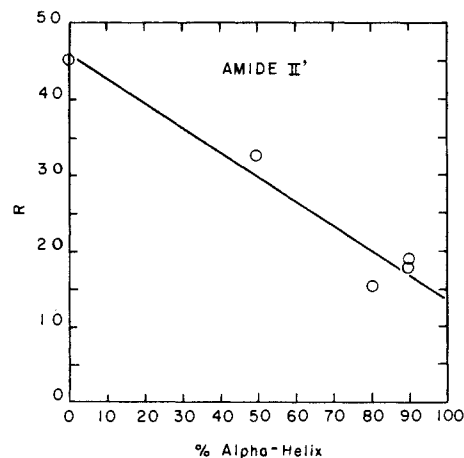


Figure 6. As Figure 3 but for the amide II' band in D<sub>2</sub>O.

Since tropomyosin contains only  $\alpha$ -helical and random coil fractions, we are dealing with a two-component system, and the molar scattering ratio can be related to the composition by

$$R = j_{\alpha}X_{\alpha} + j_{\tau}X_{\tau} \quad (2)$$

where  $X_{\alpha}$  and  $X_{\tau}$  are the mole fractions of the  $\alpha$ -helix and random coil and  $j_{\alpha}$  and  $j_{\tau}$  are their scattering coefficients, per mole of peptide. Since  $X_{\alpha} + X_{\tau} = 1$ , eq 2 can be rewritten

$$R = j_{\tau} + (j_{\alpha} - j_{\tau})X_{\alpha} \quad (3)$$

which describes the linear plots in Figures 3–6. The  $j_{\alpha}$  and  $j_{\tau}$  values obtained from the slopes and intercepts of these plots are

**Table I.** Band Frequencies and Assignments for UVRR Modes of Rabbit Muscle Tropomyosin Excited at 200 nm

pH 7	pH 9	pH 10	pH 11	pH 12.5	assignment <sup>a</sup>
			A. H <sub>2</sub> O		
981	981	981	981	981	SO <sub>4</sub>
1175	1175	1175	1175	1175	tyr
1208	1208	1208	1208	1208	tyr
1265	1265	1265	1271	1248/1299	amide III + tyr
<i>b</i>	<i>b</i>	<i>b</i>	1395	1395	?
1548	1547	1547	1551	1551	amide II
1610	1610	1596	1596	1595	tyr + phe
1648	1648	1648	1648	1657	amide I
pD 7	pD 9	pD 10	pD 11	pD 12.5	assignment <sup>a</sup>
			B. D <sub>2</sub> O		
981	981	981	981	981	SO <sub>4</sub>
1180	1180	1180	1175	<i>c</i>	tyr
1210	1210	1210	1206	<i>c</i>	tyr
1254	1254	1254	1254	<i>c</i>	tyr
1456	1457	1457	1457	1457	amide II'
<i>b</i>	<i>b</i>	<i>b</i>	1553	1553	ionized tyr
1586	1586	1587	<i>b</i>	<i>b</i>	tyr + phe
1609	1609	1610	1603	1601	tyr + phe
1648	1648	1648	1648/1660	1658	amide I'

<sup>a</sup> Assignments taken from ref 26. <sup>b</sup> Band not observed. <sup>c</sup> Band too weak to accurately assign frequency.

**Table II.** Tropomyosin Amide Band Resonance Raman Intensities and Scattering Coefficients

band	$R_7^a$	$R_9^a$	$R_{10}^a$	$R_{11}^a$	$R_{12.5}^a$	$j_\alpha^b$	$j_\tau^b$	$J_\tau/J_\alpha$
amide I	6.53	6.50	8.78	5.63	6.98	7.04	6.64	0.94
amide II	8.10	8.05	8.78	11.25	15.53	7.21	15.48	2.15
amide III	7.20	7.11	7.63	10.44	12.66	6.60	12.23	1.96
amide II'	18.99	18.37	15.70	32.92	45.95	14.01	46.58	3.32

<sup>a</sup>  $R_i$  = intensity ratio, relative to sulfate, per mole of peptide, at pH/pD *i*. <sup>b</sup> Peptide scattering coefficients for  $\alpha$ -helical and random coil conformations.

**Table III.** Estimates of  $\alpha$ -Helix Content from the 200-nm Amide II' Raman Band Intensity, Using the Tropomyosin Scattering Coefficients

protein	% $\alpha$ -helix from UVRR	% $\alpha$ -helix from X-ray or ORD
myoglobin, pD 7	81	86 <sup>a</sup>
bovine serum albumin, pD 7	58	55 <sup>b</sup>
cytochrome <i>c</i> , pD 7	34	39 <sup>c</sup>

<sup>a</sup> X-ray, from ref 26. <sup>b</sup> ORD, from ref 28. <sup>c</sup> X-ray, from ref 27.

given in Table II, along with the  $R$  values at different pH/pD.

To test the universality of these molar scattering factors, we used them to estimate via eq 3 the  $\alpha$ -helical content from UVRR spectra of two proteins with known crystal structure, myoglobin,<sup>26</sup> and cytochrome *c*,<sup>27</sup> and one protein, bovine serum albumin, whose helical content has previously been estimated via optical rotatory dispersion<sup>28</sup> measurements. The amide II' band in D<sub>2</sub>O solution was chosen for these measurements; being the dominant feature of the spectra, its intensity can be measured more reliably than that of amide II or III in H<sub>2</sub>O. The results are given in Table III and are seen to be quite satisfactory.

## Discussion

When two or more chromophores are brought close together, the interactions of their transition dipoles can lead to alterations in the positions and relative strengths of the electronic absorptions (exciton splitting). In addition, there can be an overall loss in absorption strength in one part of the spectrum due to interactions with high-lying excited states (hypochromism).<sup>29</sup> Both effects depend on the proximity and orientations of the interacting

chromophores. UV hypochromism is particularly familiar for nucleic acid duplexes, in which the stacking interactions of the purine and pyrimidine bases lead to a substantial loss in absorptivity for the characteristic UV absorption bands.<sup>30</sup> It is well-known that certain purine and pyrimidine Raman bands also show a loss in intensity when the chromophores are stacked, even though most measurements have been carried out with excitation in the visible region.<sup>31</sup> The resonance enhancement of Raman bands scales with the square of the oscillator strength of the resonant electronic transition,<sup>31</sup> so that absorption hypochromism should produce enhanced Raman hypochromism for bands that are directly in resonance with the affected electronic transition. This relationship has recently been confirmed for nucleic acids by direct excitation in the hypochromic UV absorption bands.<sup>4,32</sup> The Raman hypochromism in the visible region is believed to be due to preresonance Raman enhancement.<sup>31,33</sup>

The amide linkage is associated with a strong absorption band at  $\sim 190$  nm, which is assigned to a  $\pi$ - $\pi^*$  transition.<sup>18</sup> When a polypeptide folds into the  $\alpha$ -helical structure, this absorption shows both exciton splitting<sup>34,35</sup> and a loss in overall intensity.<sup>18-36</sup> The hypochromism seen for the 190 nm  $\pi$ - $\pi^*$  transition of  $\alpha$ -helical polypeptides is compensated for ( $\sim 80\%$ ) by hyperchromism in higher energy electronic transitions (at ca. 165-nm).<sup>37-39</sup> In the Raman spectrum, three amide vibrational bands, I-III, are of particular interest. Amide I, at  $\sim 1650$  cm<sup>-1</sup>, is predominantly C=O stretching in character, while amides II and III, at  $\sim 1550$  and  $\sim 1250$  cm<sup>-1</sup>, are mixtures of C-N stretching and N-H bending.<sup>22-24</sup> When the amide N-H proton is exchanged for a deuteron, the N-D bending mode is at much lower frequency,

(30) Voet, D.; Gratzer, W. B.; Cox, R. A.; Doty, P. *Biopolymers* **1963**, *1*, 193-208.

(31) Small, E.; Peticolas, W. L. *Biopolymers* **1971**, *10*, 69-88.

(32) Chinsky, L.; Turpin, P. V. *Biopolymers* **1980**, *19*, 1507-1515.

(33) Painter, P. C.; Koenig, J. L. *Biopolymers* **1976**, *15*, 241-255.

(34) Doty, P. *J. Polymer Sci.* **1961**, *49*, 148.

(35) Brahms, J.; Pilet, J.; Damany, H.; Chandrasekharan, V. *Proc. Natl. Acad. Sci. U.S.A.* **1968**, *60*, 1130-1137.

(36) Imahori, K.; Tanaka, J. *J. Mol. Biol.* **1959**, *1*, 359-364.

(37) Momii, R. K.; Urry, D. W. *Macromolecules* **1968**, *1*, 372-373.

(38) Bensing, J. L.; Pysh, E. S. *Chem. Phys. Lett.* **1969**, *4*, 120-122.

(39) Onari, S. *J. Phys. Soc. Jpn.* **1970**, *29*, 528.

(25) Glasoe, P. K.; Long, F. A. *J. Phys. Chem.* **1960**, *64*, 188-190.

(26) Dickerson, R. E.; Geis, I. "Hemoglobin"; Benjamin/Cummings: Menlo Park, CA., 1983; p 31.

(27) Dickerson, R. E.; Takano, T.; Eisenberg, D.; Kallai, O. B.; Samson, L.; Cooper, A.; Margoliash, E. *J. Biol. Chem.* **1971**, *246*, 1511-1535.

(28) Schechter, E.; Blout, E. R. *Proc. Natl. Acad. Sci. U.S.A.* **1964**, *51*, 695-702.

(29) Tinoco, I.; Halpern, A.; Simpson, W. T. In "Polyamino Acids, Polypeptides and Proteins"; Stahmann, M. A., Ed.; University of Wisconsin Press: Madison, 1962; pp 147-157.

leaving amide II' at  $\sim 1460\text{ cm}^{-1}$  as a nearly pure C-N stretching mode. Amides I, II, and III are all seen in UVRR spectra excited near the amide absorption band.<sup>8-12,15-17</sup> The strongest of the three is amide II; amide II' is even stronger, becoming the dominant feature of the UVRR protein spectra run in D<sub>2</sub>O (see Figure 2). Moreover, the molar scattering factors for amide II' are close to the sums of those for amides II and III (see Table II). As discussed by Hudson and co-workers,<sup>11,17</sup> this behavior implies that C-N stretching is the main distortion coordinate for the amide  $\pi-\pi^*$  excited state, which has a particularly large Franck-Condon factor for amides II and II'.

This interpretation is fully in accord with the observed Raman hypochromism, which affects the amide II, II', and III bands. Indeed the Raman intensities of these bands do scale roughly with the square of the absorption strength, as expected. Thus, Rosenheck and Doty have measured molar absorptivities for  $\alpha$ -helical and random coil peptides of 4100 and 6900 at 190 nm.<sup>18</sup> The ratio of their squares, 2.83, compares well with the ratios of the molar scattering factors for amides II, II', and III, 2.15, 3.32, and 1.96, respectively. It can be inferred that these bands gain nearly all their intensity from resonance with the 190-nm  $\pi-\pi^*$  transition. This is also the conclusion of Dudik et al.,<sup>12</sup> who found that the preresonance excitation profiles for the amide II and III bands of acetamide and *N*-methylacetamide could be accurately fit by *A* term (Franck-Condon) scattering via the  $\pi-\pi^*$  transitions. With visible wavelength excitation, far from resonance, the amide III band is weak but still shows preresonant hypochromism for  $\alpha$ -helical peptides,<sup>20,33</sup> while amide II is too weak to be observed. On the other hand, the amide I band is a strong feature of the visible Raman spectra, and the near invariance of its intensity with  $\alpha$ -helical content implies that it gains very little of its intensity from the 190-nm electronic transition. In the visible region, it actually shows increased strength for  $\alpha$ -helices, and Painter and Koenig<sup>33</sup> have suggested enhancement via the  $n-\pi^*$  transition at  $\sim 220\text{ nm}$ , which is somewhat augmented for  $\alpha$ -helices. This transition is very weak ( $\epsilon \sim 100$ ),<sup>40</sup> however, and probably does not contribute significantly to the amide I intensity at 200 nm, which no doubt derives mainly from higher lying excited states which are known to be hyperchromic for  $\alpha$ -helical polypeptides.<sup>38</sup>

Dudik et al.<sup>12</sup> found no evidence for enhancement of the C=O stretching mode of acetone, analogous to the amide I mode of peptides, at excitation wavelengths within the weak, isolated  $n-\pi^*$  absorption band at 215 nm.

Tropomyosin was chosen for this study because it exists in only two conformations,  $\alpha$ -helix and random coil,<sup>41</sup> whose fractions can be varied over a wide range by adjusting the pH.<sup>19</sup> In analyzing other proteins, one must consider the possibility that the molar scattering factors may have a range of values for different peptide conformations. The absorption studies of Rosenheck and Doty<sup>18</sup> showed that the amide absorptivity is slightly higher but nearly the same for  $\beta$ -sheet peptides as for the random coil. We expect the difference between the random coil and  $\beta$ -sheet peptides to be likewise small in the UV Raman spectrum, the  $\beta$ -sheet form perhaps showing slight hyperchromism. Thus, hypochromism appears to be a unique characteristic of the  $\alpha$ -helix. In this case, the molar scattering factors may have one set of values for  $\alpha$ -helical peptides and a narrow range of values for all other conformations. This assumption is implicit in our use of the UVRR intensities to estimate the  $\alpha$ -helical content of myoglobin, cytochrome *c*, and bovine serum albumin. These proteins span a wide range of helix contents, and the good agreement with other methods, particularly X-ray crystallography (Table III), suggests that the assumption may be reasonable. It therefore appears that the UVRR technique may offer a sensitive and relatively interference-free method for helix content determination in polypeptides and proteins.

**Acknowledgment.** This work was supported by NSF Grant CHE 8106084 and NIH Grant GM 25158.

**Note Added in Proof.** While this paper was under review, Chinsky et al.<sup>42</sup> reported preresonance Raman spectra of poly-(L-lysine) in its  $\alpha$ -helix and random coil forms and native and denatured (80 °C) ribonuclease A with 248-nm excitation. Although the authors make no mention of it, their data show clear evidence of hypochromism for the amide II and III modes associated with the  $\alpha$ -helix secondary structure (see Figures 2 and 7 of ref 42).

(40) Cantor, C. R.; Schimmel, P. R. "Biophysical Chemistry"; W. H. Freeman: San Francisco, 1980; Part II, pp 375.

(41) Talbot, J. A.; Hodges, R. S. *Acc. Chem. Res.* 1982, 15, 224-230.  
(42) Chinsky, L.; Jolles, B.; Laigle, A.; Turpin, P. Y. *J. Raman Spectrosc.* 1985, 16, 235-241.

## Ferricytochrome *b*<sub>5</sub>: Assignment of Heme Propionate Resonances on the Basis of Nuclear Overhauser Effect Measurements and the Nature of Interprotein Contacts with Partner Redox Proteins

Stuart J. McLachlan,<sup>1a</sup> Gerd N. La Mar,<sup>\*1a</sup> and Einar Sletten<sup>1b</sup>

Contribution from the Departments of Chemistry, University of California, Davis, California 95616, and University of Bergen, Bergen, Norway. Received August 5, 1985

**Abstract:** Nuclear Overhauser effect experiments have led to the stereospecific assignment of the four methylene proton pairs of the heme propionate side chains in ferricytochrome *b*<sub>5</sub>. The pH-sensitive resonances have been assigned to the exposed heme propionate on the heme pyrrole ring III. In addition it has been shown that this group is able to bind extrinsic metal ions and is intimately involved in the binding site for redox partner proteins. The patterns of the  $\alpha$ -methylene proton hyperfine shifts for both propionates are concluded to be inconsistent with the orientation obtained from available X-ray crystal coordinates and suggest specific rotations for each side chain. The nature of the slight changes resulting from complex formation with partner redox proteins such as cytochrome *c* or myoglobin is shown to be consistent with a decrease of the p*K* for the exposed 6-propionate carboxylate. This decrease supports a direct participation of this group in a salt bridge to the partner protein.

Cytochrome *b*<sub>5</sub> is found both as a membrane-bound protein in mammalian liver microsomes as well as a soluble form in eryth-

rocytes. The microsomal protein plays an important role in fatty acid desaturation<sup>2</sup> while the soluble form acts as an electron